

1 **Future Projections of Extreme Storm Tides and Related Coastal Flooding**  
2 **along the Greek Coastal Zone under Climate Change Scenarios**

3 Christos Makris<sup>1</sup>, Panagiota Galiatsatou<sup>2</sup>, Yannis Androulidakis<sup>3</sup>, Zisis Mal-  
4 lios<sup>4</sup>, Vasilis Baltikas<sup>4</sup>, Yannis Krestenitis<sup>4</sup>

5 <sup>1</sup> Democritus University of Thrace, Dept. of Civil Engineering, 67100 Xanthi,  
6 Greece

7 <sup>2</sup> EYATH S.A., 54621 Thessaloniki, Greece

8 <sup>3</sup> University of the Aegean, Dept. of Marine Sciences, 81100 Mytilene,  
9 Greece

10 <sup>4</sup> Aristotle University of Thessaloniki, Dept. of Civil Engineering, 54124  
11 Thessaloniki, Greece  
12 cmakris@civil.duth.gr

13 **Abstract.** The intensifying threat of coastal flooding due to cli-  
14 mate change calls for robust modelling and site-specific projec-  
15 tions of extreme storm surge events combined with estimations of  
16 Sea Level Rise (SLR) and astronomical tides. Greece, with over  
17 15,000 km of coastline and several low-lying littoral zones, is par-  
18 ticularly vulnerable to such hazards. This study aims to assess the  
19 projected impact of climate change on the magnitude and fre-  
20 quency of extreme storm surges across key coastal areas in Greece,  
21 through the integration of a) large-scale modelled coastal sea level  
22 dynamics and historical tide-gauge records, and b) high-resolution  
23 Digital Terrain Models (DTM) and fine-scale hydraulic flood  
24 modelling simulations.

25 A hybrid methodology combining Extreme Value Analysis (EVA)  
26 for storm-induced sea levels with physics-based hydrodynamic in-  
27 undation modelling (CoastFLOOD) was applied in several ex-  
28 posed areas along the Greek coastal zone. The case studies refer to  
29 both natural beaches in low-lying rural coastal environments and  
30 engineered waterfronts in urban areas. Coastal sea-level input for  
31 flood-hazard scenario simulations was constructed using GEV-  
32 based return levels (e.g., 50-, 100-, 500-, and 1000-year), includ-  
33 ing future SLR contributions and local characteristics of astronomi-  
34 cal tides, based on Representative Concentration Pathways (RCP)  
35 4.5 and 8.5. Graphical outputs include maps of flood extents,

36 characteristic floodwater depths and velocities, inundation hazard  
37 indices and curves, and several flood exposure metrics.

38 Our simulations reveal substantial increases in flood extent and  
39 intensity under future scenarios, mainly affected by potentially in-  
40 creasing SLR towards the end of the 21<sup>st</sup> century, especially in  
41 low-land urbanised zones. For the standard 100-year return level  
42 of storm tides, combined with SLR, floodwater inundation is pro-  
43 jected to reach critical infrastructure, residential zones, and  
44 transport pathways. Furthermore, a preliminary exposure assess-  
45 ment indicates that coastal properties in certain areas may be af-  
46 fected under worst-case scenarios, underscoring the need for up-  
47 dated zoning and adaptive planning.

48 These findings emphasise the need for integrating future storm  
49 surge extremes into locally implemented flood risk management,  
50 real estate and insurance valuation, socioeconomic impact assess-  
51 ment, and protection schemes in Greek coastal areas. The pro-  
52 posed methodological framework provides a reproducible ap-  
53 proach for similar evaluations in other Mediterranean coastal re-  
54 gions facing flood threats.

55 **Keywords:** Coastal Inundation, Storm Surge, Sea Level Rise,  
56 Extreme Value Analysis, Greece.

## 57 **1 Introduction**

58 Coastal zones worldwide are increasingly exposed to the combined effects of  
59 mean sea-level rise (MSLR), changes in storminess, and anthropogenic pres-  
60 sures. In semi-enclosed basins such as the Mediterranean Sea, storm surges and  
61 wave storms, superimposed on rising mean sea level (MSL), can generate a  
62 total water level (TWL) that may threaten coastal communities, critical infra-  
63 structure, and ecosystems. Greece, with over 15,000 km of coastline and many  
64 densely populated, low-lying littoral areas, is particularly vulnerable to episodic  
65 coastal flooding driven by extreme storm-tide events.

66 Recent studies have shown that storm surge maxima in the Mediterranean  
67 exhibit substantial regional variability due to complex basin geometry, variable  
68 bathymetry, shifts in cyclogenesis centres, the distribution of cyclonic tracks,  
69 and the influence of deep depressions [1]. At the same time, long-term changes  
70 in storminess under climate change are not spatially uniform; several studies  
71 report a general attenuation of surge extremes over large parts of the basin, but  
72 with local increases at specific gulfs, bights, and coastal inlets [2]. Such nu-  
73 anced patterns underscore the need for regional-to-local-scale assessments that

74 translate large-scale climate signals into site-specific coastal flood-hazard pro-  
75 jections [3,4].

76 For the design of engineering flood protection and coastal risk management,  
77 extreme total water levels with specified return periods are typically estimated  
78 using Extreme Value Analysis (EVA) applied to historical or modelled sea-  
79 level records. The Generalised Extreme Value (GEV) distribution and the  
80 Peaks-Over-Threshold approach have been widely used in coastal applications  
81 to estimate return levels of storm surge and wave heights [5,6]. In a changing  
82 climate, however, the uncertainty is prevalent; thus, modelling chains must in-  
83 tegrate ensemble climate projections with hydrodynamic and statistical meth-  
84 ods to derive future design conditions at the shoreline.

85 In parallel, numerical modelling of overland flooding has advanced signifi-  
86 cantly. While several complete shallow-water equation solvers provide full hy-  
87 drodynamic simulations, reduced-complexity approaches (e.g., LISFLOOD  
88 and SFINCS) based on rasterised, mass-balance, Manning-type formulations  
89 have become very popular for large-scale applications, owing to their compu-  
90 tational efficiency and ability to handle very high spatial-resolution digital ele-  
91 vation models (DEMs) [7,8]. The CoastFLOOD model [9] belongs to this cat-  
92 egory and has been applied to a range of coastal inundation problems in Greece  
93 and the US.

94 This contribution presents a hybrid framework designed to quantify future  
95 changes in extreme storm tides and associated coastal flooding along the Greek  
96 coastal zone under certain climate change scenarios. The specific objectives are  
97 to: (i) use atmospheric input from MED-CORDEX climate simulations [10,11]  
98 as input to feed MeCSS model runs for storm surges/tides [1]; (ii) derive en-  
99 semble projections of extreme sea levels at the shoreline based site-specific  
100 EVA [12]; (iii) transform these drivers into high-resolution flood hazard maps  
101 (extent, height, velocity, intensity) for several representative Greek coastal sites  
102 using high-resolution CoastFLOOD model simulations [9]; (iv) synthesise the  
103 results in terms of a Coastal Inundation Hazard Index (CIHI) ranking [13]; and  
104 (v) discuss implications for climate-resilient coastal management.

## 105 **2 Methods and Data**

106 The proposed methodology integrates regional climate projections, storm surge  
107 modelling, extreme value statistics, and reduced-complexity coastal flooding  
108 simulations applied along the entire coastline of Greece, with a focus on 20  
109 characteristic littoral regions across the Aegean, Ionian, and Cretan Seas. It pro-  
110 ceeds in four main steps: (1) storm-surge simulations for the Mediterranean Sea  
111 using the MeCSS model driven by Regional Climate Model (RCM) outputs;  
112 (2) extraction of annual maxima for storm-induced Sea Surface Heights (SSH)  
113 and EVA at littoral grid points along the Greek coasts; (3) construction of

114 location-specific total water-level scenarios by adding maximum astronomical  
115 tidal ranges and projected MSLR; and (4) CoastFLOOD inundation simulations  
116 for a set of representative Greek coastal sites under present and future extreme  
117 forcing.

118 Storm surges are simulated using the Mediterranean Climate Storm Surge  
119 (MeCSS) model, a depth-averaged barotropic hydrodynamic model based on  
120 the shallow-water equations. MeCSS solves for water levels and depth-aver-  
121 aged currents on a curvilinear grid covering the entire Mediterranean basin,  
122 with open boundaries prescribed at the Strait of Gibraltar and Marmara [1]. At-  
123 mospheric forcing consists of 10 m wind components and sea-level pressure  
124 fields from three high-resolution MED-CORDEX RCMs: CMCC-CCLM,  
125 CNRM-ALADIN, and GUF-CCLM-NEMO. Simulations are conducted for a  
126 historical reference period (1971–2005) and two 35-year future periods (STF:  
127 2021–2055; LTF: 2066–2100) under RCP4.5 and RCP8.5 [1, 10, 11]. For each  
128 coastal grid cell, the storm-induced SSH time series is extracted and high-pass  
129 filtered to remove low-frequency signals not related to meteorological forcing.

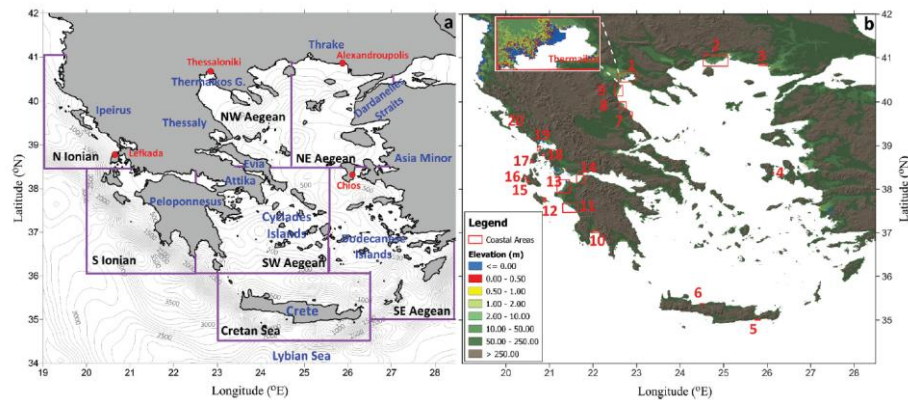
130 EVA is applied to the annual maximum storm-induced SSH series at each  
131 littoral grid cell. The GEV distribution is selected because it represents the lim-  
132 iting distribution of block maxima under general conditions [14]. The cumula-  
133 tive distribution function is defined by the location parameter  $\mu$ , the scale pa-  
134 rameter  $\sigma$ , and the shape parameter  $\xi$ , which controls the tail behaviour. Param-  
135 eter estimation is performed using the L-moments method, which has proven  
136 robust for relatively short samples (here, 35 years of annual maxima per period)  
137 [12]. For each cell, 50- and 100-year return levels of storm-induced SSH are  
138 estimated. Confidence intervals are constructed using a parametric bootstrap  
139 procedure in which synthetic samples are generated from the fitted GEV, re-  
140 fitted, and return levels re-computed to obtain empirical percentiles.

141 To combine storm surges with long-term MSLR, the derived storm-induced  
142 SSH extremes are superimposed on projected MSL changes for the correspond-  
143 ing RCP scenarios and periods. This yields location-specific TWLs that repre-  
144 sent the combined effect of surges, tides, and MSL change. These TWLs are  
145 used as offshore boundary conditions for local inundation simulations.

146 Coastal flooding is simulated using CoastFLOOD [9], a reduced-complexity  
147 two-dimensional model that solves the mass conservation equation on a regular  
148 raster grid. Water depths in each cell evolve according to the balance between  
149 incoming and outgoing discharges to neighbouring cells and local storage. Hy-  
150 draulic fluxes are computed using a decomposed Manning-type formulation  
151 driven by water-level gradients between adjacent cells. The wetting–drying al-  
152 gorithm activates or deactivates cells based on local water-depth thresholds.  
153 The computational domain covers coastal stretches of 1–20 km length and sim-  
154 ilar cross-shore extent, discretised at 2–5 m resolution, yielding simulation  
155 grids of up to about  $16 \times 10^6$  cells.

156 The necessary DEMs are derived from the Hellenic Cadastre, which provides  
 157 detailed topographic data for the coastal floodplains. Land-cover information is  
 158 taken from CORINE Land Cover (CLC) datasets, which classify Europe into  
 159 44 land-use categories. These categories are mapped to Manning roughness co-  
 160 efficients through look-up tables, and the resulting spatially variable friction  
 161 fields are used to parameterise floodplain resistance to water flow. For each  
 162 coastal site, scenarios of extreme storm-tide events are translated into time-var-  
 163 ying boundary conditions applied along the seaward edge of the domain, and  
 164 simulations are run for several hours to a few days to capture the potential max-  
 165 imum inundation buildup.

166 Twenty representative coastal sites distributed across seven Greek regional  
 167 seas are selected (Fig. 1): the northwestern, northeastern, southwestern, and  
 168 southeastern Aegean Sea, the Cretan Sea, and the northern and southern Ionian  
 169 Sea. Sites include both urbanised settings, such as Thessaloniki and the broader  
 170 Thermaikos Gulf, Alexandroupolis, and Kalamata, and more rural or touristic  
 171 locations, such as Laganas (Zakynthos), Vassiliki (Lefkada), and Ierapetra  
 172 (Crete). For each site and scenario, the spatial extent of flooding is extracted  
 173 and normalised to a reference area (the global upper threshold of inundation  
 174 area), providing input to our coastal hazard analysis.



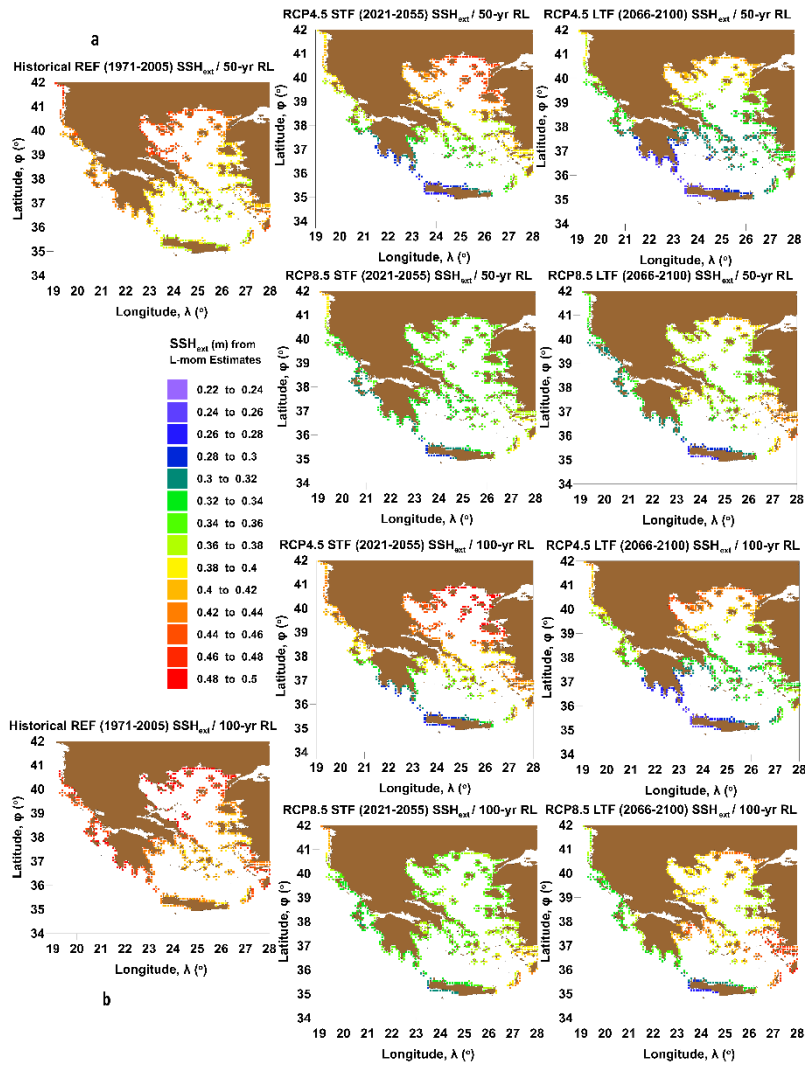
175  
 176 **Fig. 1.** Bathymetry of the study area with 7 subregions and 20 locations at the  
 177 NW Aegean, NE Aegean, SW Aegean, SE Aegean, Cretan Sea, N Ionian, and  
 178 S Ionian Sea: Thermaikos Gulf (1), Nestos (2), Alexandroupolis (3), Chios (4),  
 179 Ierapetra (Crete; 5), Rethymno (Crete; 6), Pineios (7), Agiokampos (8), Kate-  
 180 rini (9), Kalamata (10), Katakolo (11), Laganas (Zakynthos; 12), Manolada  
 181 (13), Patra (14), Argostoli (Kefalonia; 15), Livadi (Kefalonia; 16), Vassiliki  
 182 (Lefkada; 17), Palairos (18), Preveza (19), Igoumenitsa (20).  
 183

184 The CIHI is defined as a composite metric combining a ranked driver-inten-  
 185 sity term (based on the magnitude of the extreme TWL) with a ranked normal-  
 186 ised flood-area term (the ratio of flooded area to a predefined ceiling). CIHI  
 187 values are used to categorise sites into low-, moderate-, and high-hazard classes

188 under present and future conditions, and to quantify relative changes attributa-  
 189 ble to climate forcing.

## 190 3 Results

### 191 3.1 Extreme Storm Surges on the Coast



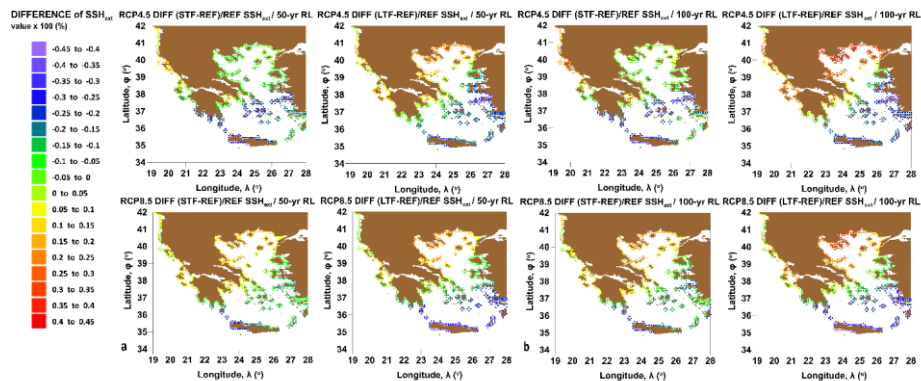
192  
 193  
 194  
 195

**Fig. 2.** Maps of 50- & 100-year RV of Extreme SSH by GUF-based MeCSS simulations during Reference, STF, LTF for RCP 4.5-8.5.

196 The GEV-based EVA of MeCSS storm-surge simulations confirms the sub-  
 197 stantial spatial variability of extreme storm-induced SSH along the study area's  
 198 coastline and, in particular, around Greece. For the historical reference period,  
 199 the highest 50- and 100-year return levels in the wider Mediterranean are found  
 200 in the northern Aegean. Along the Greek coasts, 50-year storm-surge return  
 201 levels generally range from 0.25 to 0.55 m, with the highest values occurring at  
 202 exposed gulfs with long fetches and favourable orientations relative to domi-  
 203 nant winds (Fig. 2).

204 When comparing future periods with the reference baseline, a basin-wide  
 205 attenuation of storminess is evident under both RCP4.5 and RCP8.5, particu-  
 206 larly in the 2nd half of the 21st century (Fig. 2). Percentage differences in 50-  
 207 year storm surges across the study area typically range from  $-30\%$  to  $-2\%$  by  
 208 2100. Nonetheless, this overall decrease may mask a substantial positive local  
 209 deviation in the central and northern Aegean and Ionian Seas; storm-surge ex-  
 210 tremes may increase by up to 20–30%, depending on the RCM and scenario.

211 For Greece, the ensemble of MeCSS–RCM simulations reveals a mixed pat-  
 212 tern. In several regions, particularly in the southern Aegean and parts of the  
 213 Ionian Sea, the projected reduction in storminess is expected to slightly lower  
 214 future surge extremes. In contrast, the northern Aegean, the entrance of Ther-  
 215 maikos Gulf, and some Ionian sites display modest but statistically meaningful  
 216 increases in extreme storm tides under at least one scenario–RCM combination.  
 217 When combined with MSLR, even modest changes in surge extremes can trans-  
 218 late into appreciable differences in TWLs at the coast.  
 219

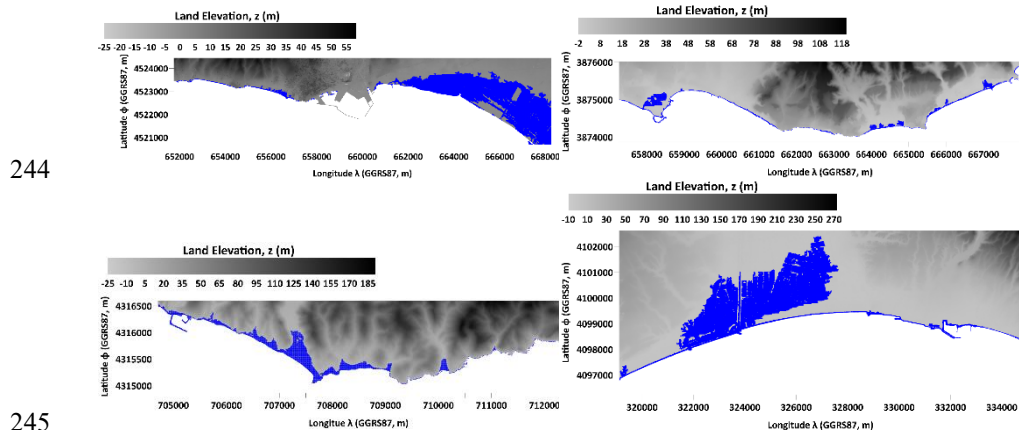


220  
 221 **Fig. 3.** Maps of Differences for 50- & 100-year RV of  $SSH_{ext}$  by CNRM-  
 222 based MeCSS simulations during Reference STF and LTF for RCP4.5-8.5.  
 223

### 224 3.2 Coastal Flooding Impacts due to several TWL Scenarios

225 CoastFLOOD simulations driven by the highest projected total water levels  
 226 translate these offshore signals into spatially explicit flood maps. For Alexan-  
 227 droupolis, located in the northern Aegean, future scenarios under the RCP8.5

228 project a clear expansion of flood extent across low-lying urban areas near the  
 229 port and the airport access roads, with flooded areas increasing by more than  
 230 15% relative to present-day conditions in the long term. In Ierapetra, on the  
 231 southern coast of Crete, steep topography restricts inland penetration, so flood  
 232 extents remain relatively limited despite elevated water levels, highlighting the  
 233 crucial role of local morphology. In western Greece, simulations for Kalamata  
 234 and Plomari illustrate different hydrodynamic behaviours. In Plomari, a narrow  
 235 coastal lowland is easily over-topped under combined surge and MSLR, and  
 236 floodwaters can propagate along the coastal plain, threatening transport corri-  
 237 dors and built-up areas. Kalamata, by contrast, exhibits hydraulic connectivity  
 238 between the shoreline and more inland depressions, so storm tides can activate  
 239 complex flow pathways that inundate areas not directly adjacent to the sea. At  
 240 several sites, projected changes in the area affected by flooding under RCP8.5  
 241 by 2100 fall within the range of 10–20%, whereas in other locations they remain  
 242 within a few per cent, consistent with local attenuation of storminess.  
 243



245  
 246 **Fig. 4.** Flood Extents (FA) with CoastFLOOD simulations driven by the highest  
 247 extreme TWL in Alexandroupoli (N Greece), Plomari (W Greece), Kalamata  
 248 (SE Greece), Ierapetra (S Greece) from left to right and top to bottom.  
 249

### 250 3.3 Results

251 The CIHI provides a synthetic view of these results by ranking all 20 sites  
 252 according to combined driver intensity and flood response. Under historical  
 253 conditions, the highest CIHI values correspond to low-lying deltas, embay-  
 254 ments, and back-barrier plains with extensive urbanisation or critical assets. In  
 255 the long-term future under RCP8.5, several of these sites experience an upward  
 256 shift in hazard class, while a few locations with currently moderate hazard move  
 257 into the high-hazard category. Conversely, a limited number of sites with

258 favourable topography and reduced storminess exhibit stable or slightly re-  
259 duced CIHI values.

260 Overall, the analysis reveals that the combined effect of changing storm  
261 surges and sea-level rise is highly site-specific (Table 1). The spatially coherent  
262 patterns associated with atmospheric deep depressions and Mediterranean cy-  
263 clone tracks interact with local coastal morphology and land-use to produce a  
264 rich spectrum of future flood responses along the Greek coastline.  
265

266 **Table 1.** Characteristic CIHI values for hazard severity by combining ranked  
267 driver (storm tide) intensity with a ranked Normalised Inundation Index  
268 (Flooded Fraction),  $FA_{\text{ext}}/FA_{\text{ceiling}}$ .

A/A	Ierapetra	Rethymno	Kalamata	Katakolo	Argostoli	Livadi
MAX	1.061	0.902	1.273	1.105	1.057	1.059
RANK	12	22	3	10	14	13
CIHI	5	5	1	5	1	1
A/A	Patra	Chios	Vasiliki	Palairos	Plomari	Kyparissia
MAX	1.105	0.974	1.042	1.055	1.222	1.138
RANK	11	18	16	15	5	7
CIHI	2	3	2	1	-	-

## 269 4 Discussion

270 The results confirm that climate change affects storm surges and coastal flood-  
271 ing in the Mediterranean in ways that simple monotonic trends cannot summa-  
272 rise. Instead, they emerge from a combination of (i) large-scale modifications  
273 in the frequency, intensity, and tracks of deep depressions and cyclones, (ii)  
274 regional sea-level rise, and (iii) local coastal morphology and human occupa-  
275 tion. The projected basin-wide attenuation of storm surges in many regions re-  
276 flects a likely northward shift and reorganisation of atmospheric circulation pat-  
277 terns. Yet, local hotspots of intensification persist, where topographic and bath-  
278 ymetric configurations favour surge amplification. Specifically, a comparison  
279 of positive versus negative differences in extreme Flood Extents ( $FA_{\text{ext}}$ ) at se-  
280 lected Greek coastal sites is presented in Table 2, based on several combinations  
281 of climatic scenarios, RCPs, RCMs, and Return-Periods (RPs). Positive  
282 changes are few but, conditionally, exceed the 5% significance threshold.

283 For infrastructure designers and coastal planners, this implies that relying  
284 solely on basin-average or global sea-level rise projections is insufficient for  
285 robust risk assessments. Instead, detailed regional modelling of storm surges,  
286 combined with extreme value statistics and high-resolution inundation simula-  
287 tions, is required to identify the most critical sites and to quantify the range of  
288 possible future outcomes. The hybrid framework presented here offers such a

289 pathway by linking MED-CORDEX RCM outputs, MeCSS surge simulations,  
290 EVA, and CoastFLOOD at representative Greek sites.

291

292 **Table 2.** Positive vs. negative differences of extreme Flood Extents ( $FA_{ext}$ ) at  
293 selected Greek coastal sites based on combinations of climatic scenarios RCPs,  
294 RCMs, Return-Periods RPs. Positive changes are marked in bold.

RCP/ Future	RCM	RP (years)	Ierapetra	Rethymno	Kalamata	Laganas	Thermaikos
RCP45- STF	CMCC	50	-2.03%	<b>1.51%</b>	-0.50%	<b>2.12%</b>	<b>2.70%</b>
		100	0.00%	<b>2.93%</b>	-0.39%	<b>2.13%</b>	<b>1.71%</b>
	CNRM	50	-6.26%	-11.64%	-5.74%	-2.88%	-0.98%
		100	-5.65%	-11.24%	-5.80%	-2.78%	<b>0.40%</b>
	GUF	50	-11.47%	-10.51%	-7.82%	-8.14%	-1.17%
		100	-11.55%	-13.97%	-9.13%	-12.45%	-2.15%
RCP45- LTF	CMCC	50	-4.15%	-5.42%	<b>0.77%</b>	<b>3.48%</b>	-1.41%
		100	-3.05%	-6.33%	<b>1.17%</b>	<b>5.01%</b>	-3.23%
	CNRM	50	-12.88%	-8.51%	<b>0.14%</b>	<b>3.21%</b>	<b>4.51%</b>
		100	-11.20%	-10.42%	<b>1.19%</b>	<b>5.40%</b>	<b>8.82%</b>
	GUF	50	-14.23%	-12.75%	-9.54%	-8.80%	-1.83%
		100	-15.25%	-14.39%	-10.30%	-12.09%	-2.28%

295

296 The proposed CIHI is a pragmatic tool for synthesising complex information  
297 into a form accessible to decision-makers. By combining ranked contributions  
298 from extreme total water levels and normalised flood extents, CIHI simplifies  
299 the communication of hazard severity and its evolution under climate change.  
300 However, CIHI should be interpreted alongside complementary indicators cap-  
301 turing exposure and vulnerability, such as population density, economic value  
302 of assets, critical infrastructure, and ecosystem services, to derive compre-  
303 hensive risk indices.

304 From the perspective of the United Nations Sustainable Development Goals  
305 (SDGs), the findings have direct implications for SDG 11 (Sustainable Cities  
306 and Communities) and SDG 13 (Climate Action). Coastal municipalities with  
307 increasing CIHI values will need to integrate future storm-tide-driven flood  
308 hazards into spatial planning, building codes, emergency preparedness, and in-  
309 surance schemes. Adaptation options may range from nature-based solutions,  
310 such as wetland restoration and beach nourishment, to engineered defences and  
311 managed retreat in the most exposed locations. The analysis also supports SDG  
312 9 (Industry, Innovation and Infrastructure) by providing the quantitative basis  
313 for climate-resilient design of ports, transport links, and water-related infra-  
314 structure along the Greek coastline.

315 The study has several limitations that point to future research needs. First,  
316 while the GEV-based EVA assumes stationarity within each 35-year window,  
317 non-stationary approaches that explicitly incorporate time-varying covariates  
318 could provide additional insight, especially for mid- to long-term planning. Sec-  
319 ond, the analysis focuses on storm surges and mean sea-level rise, whereas  
320 wave setup, runup, and coincident river discharges are treated implicitly or ne-  
321 glected. Extending the framework to account for fully coupled flooding by in-  
322 tegrating coastal surge and waves with fluvial and pluvial models would yield  
323 a more comprehensive representation of coastal compound flood hazards.  
324 Third, uncertainties associated with climate model ensembles, emission path-  
325 ways, and local topographic data should be quantified more explicitly through  
326 systematic sensitivity and probabilistic analyses.

327 Despite these limitations, the present work demonstrates the feasibility and  
328 value of downscaling Mediterranean-scale climate information to the local  
329 scale of individual Greek coastal communities. The combination of physically  
330 based modelling and statistical analysis provides a consistent framework that  
331 can be updated as new climate scenarios, RCM simulations, and higher-quality  
332 topographic data become available.

## 333 5 Conclusions

334 A hybrid framework has been presented to assess future extreme storm tides  
335 and associated coastal flooding along the Greek coastal zone under climate  
336 change scenarios. The approach combines MED-CORDEX climate projec-  
337 tions, MeCSS storm-surge simulations, GEV-based EVA, and reduced-com-  
338 plexity CoastFLOOD inundation modelling at high spatial resolution for twenty  
339 representative Greek coastal sites.

340 The results indicate that, while a general attenuation of storm surges is pro-  
341 jected over large parts of the Mediterranean basin by the end of the twenty-first  
342 century, several Greek hotspots may experience local increases in extreme  
343 storm-tide levels and flood extents when storm surges are superimposed on  
344 mean sea-level rise. Projected changes in flood impacts range from negligible  
345 to more than 20% under RCP8.5 in the long term (not shown here for brevity),  
346 depending on location, coastal morphology, and atmospheric forcing.

347 The Coastal Inundation Hazard Index (CIHI) introduced in this study pro-  
348 vides a valuable synthesis of driver intensities and flood responses, offering a  
349 transparent means to compare hazard levels across sites and scenarios. The  
350 methodology and results can directly support coastal risk assessments, adapta-  
351 tion strategies, and investment planning aligned with the objectives of SDGs 9,  
352 11, and 13.

353 Future work will focus on extending the framework to account for compound  
354 flooding fully, incorporating wave effects and river discharge, refining non-

355 stationary statistical models of extremes, and integrating exposure and vulner-  
356 ability data to derive comprehensive coastal risk indices for Greece and the  
357 wider eastern Mediterranean.

## 358 **References**

- 359 1. Makris, C.V., Tolika, K., Baltikas, V.N., Velikou, K., Krestenitis, Y.N.:  
360 The impact of climate change on the storm surges of the Mediterranean Sea:  
361 coastal sea level responses to deep depression atmospheric systems. *Ocean*  
362 *Modelling* 181, 102149 (2023).
- 363 2. Conte, D., Lionello, P.: Characteristics of large positive and negative surges  
364 in the Mediterranean Sea and their attenuation in future climate scenarios.  
365 *Global and Planetary Change* 111, 159–173 (2013).
- 366 3. Lionello, P., Conte, D., Reale, M.: The effect of cyclones crossing the Med-  
367 iterranean region on sea level anomalies on the Mediterranean Sea coast.  
368 *Natural Hazards and Earth System Sciences* 19(7), 1541–1564 (2019).
- 369 4. Šepić, J., Vilibić, I., Jordà, G., Marcos, M.: Mediterranean sea level forced  
370 by atmospheric pressure and wind: variability of the present climate and  
371 future projections for several period bands. *Global and Planetary Change*  
372 86, 20–30 (2012).
- 373 5. Calafat, F.M., Wahl, T., Tadesse, M.G., Sparrow, S.N.: Trends in Europe  
374 storm surge extremes match the rate of sea-level rise. *Nature* 603, 841–845  
375 (2022).
- 376 6. Cid, A., Menéndez, M., Castanedo, S., Abascal, A.J., Méndez, F.J., Medina,  
377 R.: Long-term changes in the frequency, intensity and duration of extreme  
378 storm surge events in southern Europe. *Climate Dynamics* 46(5), 1503–  
379 1516 (2016).
- 380 7. Sharifian, M. K., Kesserwani, G., Chowdhury, A. A., Neal, J., Bates, P.:  
381 LISFLOOD-FP 8.1: New GPU accelerated solvers for faster fluvial/pluvial  
382 flood simulations. *Geoscientific Model Development Discussions* 16(9),  
383 2391–2413 (2023).
- 384 8. Leijnse, T., van Ormondt, M., Nederhoff, K., & van Dongeren, A.: Model-  
385 ing compound flooding in coastal systems using a computationally efficient  
386 reduced-physics solver: Including fluvial, pluvial, tidal, wind-and wave-  
387 driven processes. *Coastal Engineering* 163, 103796 (2021).
- 388 9. Makris, C., Mallios, Z., Androulidakis, Y., Krestenitis, Y.: CoastFLOOD:  
389 A High-Resolution Model for the Simulation of Coastal Inundation Due to  
390 Storm Surges. *Hydrology*, 10(5), 103 (2023).
- 391 10. Ruti, P.M., et al.: MED-CORDEX initiative for Mediterranean climate  
392 studies. *Bulletin of the American Meteorological Society* 97(7), 1187–1208  
393 (2016).

- 394 11. Reale, M., Cabos Narvaez, W.D., Cavicchia, L., Conte, D., Coppola, E.,  
395 Flaounas, E., Giorgi, F., Gualdi, S., et al.: Future projections of Mediterra-  
396 nean cyclone characteristics using the Med-CORDEX ensemble of coupled  
397 regional climate system models. *Climate Dynamics*, 1–24 (2021).
- 398 12. Galiatsatou, P., Makris, C., Baltikas, V., Krestenitis, Y., Prinos, P.: Analy-  
399 sis of extreme storm surges at the Mediterranean coastline under climate  
400 change. In Karambas T., Loukogeorgaki, E. (eds.) 2<sup>nd</sup> International Scien-  
401 tific Conference on Design and Management of Port Coastal and Offshore  
402 Works (DMPCO), vol. 1, pp. 36-40 (2023).
- 403 13. Androulidakis, Y., Makris, C., Mallios, Z., Krestenitis, Y.: Sea level varia-  
404 bility and coastal inundation over the northeastern Mediterranean Sea.  
405 *Coastal Engineering Journal*, 65(4), 514-545 (2023).
- 406 14. Coles, S.: *An Introduction to Statistical Modeling of Extreme Values*.  
407 Springer, London (2001).